Proceedings of the ASME 2010 3rd Joint US-European Fluids Engineering Summer Meeting and 8th International Conference on Nanochannels, Microchannels, and Minichannels
FEDSM-ICNMM2010
August 1-5, 2010, Montreal, Canada

FEDSM-ICNMM2010-30734

NUMERICAL SIMULATION OF ELECTROSTATIC ATOMIZATION IN SPINDLE MODE

Mohammad Passandideh Fard
Associate Professor, Department of Mechanical Engineering
Ferdowsi University of Mashhad, Iran
mpfard@um.ac.ir

Mohammad Reza Mahpeykar
Associate Professor, Department of Mechanical Engineering
Ferdowsi University of Mashhad, Iran
mahpeymr@ferdowsi.um.ac.ir

Sajad Pooyan
M.Sc. Student, Department of Mechanical Engineering
Ferdowsi University of Mashhad, Iran
Sajad.pooyan@gmail.com

Mortaza Rahimzadeh
M.Sc. Student, Department of Mechanical Engineering
Ferdowsi University of Mashhad, Iran
Mortaza_rahimzadeh@yahoo.com

ABSTRACT

The behavior of a liquid jet in an electrostatic field is numerically simulated. The simulations performed correspond to a transient liquid jet leaving a capillary tube maintained at a high electric potential. The surface profile of the deforming jet is defined using the VOF scheme and the advection of the liquid free surface is performed using Youngs' algorithm. Surface tension force is treated as a body force acting on the free surface using continuum surface force (CSF) method. To calculate the effect of the electric field on the shape of the free surface, the electrostatic potential is solved first. Next, the surface density of the electric charge and the electric field intensity are computed, and then the electric force is calculated. Liquid is assumed to be a perfect conductor, thus the electric force only acts on the liquid free surface and is treated similar to surface tension using the CSF method. To verify the simulation results, a simplified case of electrowetting phenomenon is simulated and free surface shape in stable state is compared with experimental results. Then the electrostatic atomization in spindle mode is simulated and the ability of the developed code to simulate this process is demonstrated.

INTRODUCTION

Electrostatic atomization, also called Electrospray, is a well known phenomenon, in which an electrostatic force elongates the liquid meniscus formed at the outlet of a capillary nozzle to a jet which next disrupts into small droplets by electrical and mechanical forces.

Electrospray systems have several advantages over mechanical atomizers. The size of electrospray drops can range from hundreds of micrometers down to several tens of nanometers. The size distribution of the droplets can be nearly monodisperse. Droplet generation and droplet size can be controlled roughly via the control of the flow rate of the liquid and the applied voltage at the capillary nozzle. The fact that the droplets are electrically charged facilitates the control of their motion (including their deflection and focusing) by means of an electric field. Charged droplets are self-dispersing in space, also resulting in the absence of droplet coagulation. The deposition efficiency of a charged spray on an object is higher than that of an uncharged spray. This feature can be utilized, for example, in surface coating or thin film production.

Electrospray has opened new routes to nanotechnology. It is used for micro- and nano-thin film deposition, micro or nano-particle production, and micro- or nano-capsule formation. Thin films and fine powders are (or potentially could be) used in modern material technologies, microelectronics, and medical technology [1]. In spite of these advantages, this method of atomization has some difficulties to perform. The main difficulty is the existence of many different atomization modes depending on the settings of the process. Jaworek et al. [2] classified ten modes of atomization according to geometrical forms of the meniscus and/or jet. Therefore numerical simulation is an effective method to understand and control the phenomenon.

Much research is contributed to the understanding of the phenomenon by modeling and simulating the involved

processes numerically. Hartman et al. [3] developed a Lagrangian model to predict the droplet size and velocity and compared the results with experiments. They also developed a physical model to obtain the shape of the liquid cone and jet; the electric field inside and outside the cone; and the surface charge density on the liquid surface [4]. In their model, a one-dimensional momentum equation was used to simulate the flow field. They claimed that the space charge due to the charged droplets has an influence of about 5 to 7% on the electric field at the cone surface. Hartman et al. [5] also used an analytical model for jet break-up and found that the jet break-up mechanism depends on the ratio of electric normal stress to surface tension stress.

Alfonso et al. [6] modeled electrospray using a hybrid experimental-numerical technique. They proved that the surface charges are always in equilibrium, being the liquid bulk quasi-neutral. They presented a consistent general scaling of all EHD variables involved, which are verified by experiments. Fang et al. [7] used a model similar to Hartman's one but solved the axisymmetric flow equations and used an adaptive grid generation scheme. Their model didn't consider jet break-up. Jun Zeng et al. [8] used a VOF method to simulate Taylor cone formation. While previous models could only predict the steady shape of the cone-Jet, by utilizing this VOF method, Zeng could capture the transition process as well. However, they didn't consider jet break-up and droplet formation; they also used a semi conductor liquid in their simulations. Orest Lastow et al. [9] performed a simulation similar to Zeng, but they studied conductive fluid atomization. They also didn't consider jet break-up and surface tension.

According to what mentioned above, most of the previous works are focused on the investigation of the cone-jet mode and spindle mode is a relatively new matter of interest. Since the conditions under which this mode occurs are very close to those of cone-jet mode the spindle mode can be assumed the transient form of the cone-jet mode. Most of the works studying the spindle mode have been experimental and they have used simplified quasistatic models. In this work the spindle mode is simulated dynamically using the volume of fluid method.

PROBLEM GEOMETRY

The configuration of the problem is depicted in Figure 1 and the dimensions of the parts pointed at by alphabetic indexes are cited at the last column of "Table 1".

A conductive liquid jet leaves a capillary nozzle with a constant volumetric flow rate and a constant electric voltage is applied between nozzle and counter electrode.

GOVERNING EQUATIONS

Fluid Flow

The fluid flow is assumed to be incompressible, axisymmetric, Newtonian and laminar. Since the air surrounding the liquid is not being forced and its viscosity is significantly less than that of liquid, it does not considerably affect any liquid motion. Therefore, only the liquid phase is considered. The mass and momentum conservation equations are as follows:

$$\vec{\nabla}.\vec{V} = 0 \tag{1}$$

$$\frac{\partial \vec{V}}{\partial t} + \vec{\nabla}.(\vec{V}\vec{V}) = -\frac{1}{\rho}\vec{\nabla}p + \frac{1}{\rho}\vec{\nabla}.\overleftrightarrow{\tau} + \vec{g} + \frac{1}{\rho} + \vec{F}_b \tag{2}$$

in which, $\vec{V}$, ρ, p and $\overleftrightarrow{\tau}$ represent the velocity vector, the liquid density, the pressure, and the stress tensor respectively. $\vec{g}$ is the gravitational acceleration and $\vec{F}_b$ is any body force (per unit volume) acting on the fluid. As the fluid is Newtonian the stress tensor is:

$$\overleftrightarrow{\tau} = \mu\left[(\vec{\nabla}\vec{V}) + (\vec{\nabla}\vec{V})^T\right] \tag{3}$$

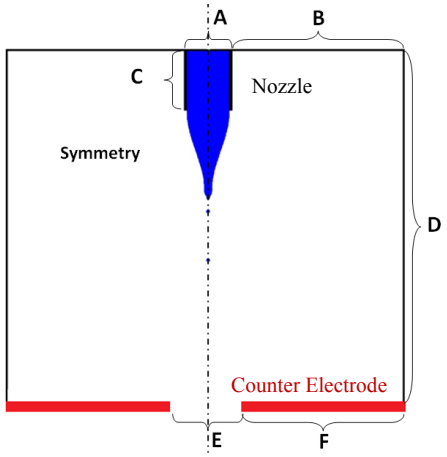

Figure 1: Configuration of the physical model. Electric potential is applied between the nozzle and the counter electrode. (Figure is not to scale.)

Above equations are solved in order to obtain the flow field. In addition, VOF scheme is used to locate the free surface position. In this method, a scalar function f, called volume fraction, is defined as the fraction of a cell volume which is occupied by the liquid. f is assumed to be unity when a cell is fully occupied by the fluid and zero for an empty cell. Cells with f values of $0 < f < 1$ define the location of the free surface. Solving the advection equation for volume fraction as follows,

$$\frac{\partial f}{\partial t} + (\vec{V}.\nabla)f = 0 \tag{4}$$

gives the f field in each time step.

Electrostatic

Along with the hydrodynamic equations presented above, the Laplace equation [10] is solved on the entire domain to calculate the electric potential in every grid cell at each time step:

$$\nabla^2\phi = 0 \tag{5}$$

In addition, the relation between the electric potential and electric field intensity is known to be:

$$\vec{E} = -\nabla\phi \tag{6}$$

Since the liquid is assumed to be a perfect conductor, the electrostatic force only acts on the liquid free surface [11]. The electrostatic force per unit area is computed as [12]:

$$\vec{F_e} = \frac{1}{2}\rho_s \vec{E} \quad (7)$$

Where ρ_s is the surface density of the electric charge and is calculated as:

$$\rho_s = -\epsilon_{Air}\vec{E}.\hat{n} = -\epsilon_{Air}\frac{\partial\phi}{\partial\vec{n}} \quad (8)$$

Where $\hat{n}$ is unit vector normal to the free surface and $\frac{\partial}{\partial\vec{n}}$ represents the gradient along the outward normal to the liquid free surface.

BOUNDARY CONDITIONS

A Neumann condition is used for the pressure in all domain boundaries ($\frac{\partial p}{\partial\vec{n}} = 0$). Also, an outflow boundary condition is used for velocity on all boundaries except on walls and at the entry of the nozzle where constant velocity is employed. A summary of boundary conditions are mentioned in "Table 1". In this table Q is the volumetric flow rate of the liquid at the nozzle inlet and ϕ_0 is the applied electric potential to the nozzle.

Table 1: Summary of applied boundary conditions based on the schematic shown in Figure 1.

	Velocity	Pressure	potential	mm
A	$v = {}^{Q}/_{A}$	${}^{\partial P}/_{\partial\vec{n}=0}$	$\phi = \phi_0$	0.51
B	${}^{\partial u}/_{\partial\vec{n}=0}$, ${}^{\partial v}/_{\partial\vec{n}=0}$	${}^{\partial P}/_{\partial\vec{n}=0}$	${}^{\partial\phi}/_{\partial\vec{n}=0}$	10.0
C	$u = 0, v = 0$	${}^{\partial P}/_{\partial\vec{n}=0}$	$\phi = \phi_0$	5.0
D	${}^{\partial u}/_{\partial\vec{n}=0}$, ${}^{\partial v}/_{\partial\vec{n}=0}$	${}^{\partial P}/_{\partial\vec{n}=0}$	${}^{\partial\phi}/_{\partial\vec{n}=0}$	15.0
E	${}^{\partial u}/_{\partial\vec{n}=0}$, ${}^{\partial v}/_{\partial\vec{n}=0}$	${}^{\partial P}/_{\partial\vec{n}=0}$	${}^{\partial\phi}/_{\partial\vec{n}=0}$	6.0
F	$u = 0, v = 0$	${}^{\partial P}/_{\partial\vec{n}=0}$	$\phi = 0$	7.25

It is important to note that the electric potential of the points within the main flow is equal to the applied potential as a result of the perfect conductor assumption for the l.

The fluid used in this work is ' Water-Methanol 50% (V/V)' which its physical properties are listed in "Table 2".

Table 2: Physical properties of (water + 0.005 % NaCl)

Density $\rho\ \left(\frac{Kg}{m^3}\right)$	Viscosity $\mu(Pa.s)$	Surface tension $\gamma\ ({}^{N}/_{m})$
894	0.0018	0.036

NUMERICAL PROCEDURE

The Youngs algorithm [13] is used for advection of function *f*. This algorithm consists of two steps: an approximate construction of the free surface and the advection of the interface to a new location. First the interface is reconstructed by locating a line within each interfacial cell utilizing the volume fraction of the cell, *f*, and the normal vector to the interface; normal vectors are computed using *f* function gradients in two directions. In the second step the reconstructed interface and new velocities are used to compute volume fluxes across each cell face in one coordinate direction at a time. Having calculated the advection of the interface in all directions, we can compute the final volume fraction field and the new shape of the interface

Surface tension is modeled as a volume force acting on fluid elements near the free surface; the method used is the continuum surface force (CSF) model [14] integrated with smoothed values of function *f* in evaluating free surface curvature [15].

The time discretization of the momentum equation is divided into two steps. First, an interim velocity is computed explicitly from convective, viscous, gravitational, and body forces for a time step Δt. Then, the pressure is calculated implicitly. As momentum cannot be advected more than a grid per time step, the Courant number should be less than one. The same condition applies for the volume tracking as it can be only advected to the neighboring cells. Further details of the solution procedure of the hydrodynamic equations using VOF method is given elsewhere [15].

The solution of the electrostatic equations in order to obtain the electrostatic force distribution on the free surface is new in this work and will be explained in details here. Some difficulties arise from constant electric potential throughout the main liquid jet. It means that the free surface of the liquid is a Dirichlet condition as the value of the electric potential on the free surface is known and set to be that of the nozzle. The deforming liquid interface may have any arbitrary shape that doesn't necessarily coincide with the edges of the computational cells. To resolve this issue we use 5 neighboring nodes in different locations with respect to the reconstructed interface to discrete the Laplace equation, Eqn. (5), near the free surface. These nodes near the free surface are schematically illustrated in Figure 2.

By employing a non-uniform Cartesian mesh, Eqn. (5) may be discretized as follows:

$$\frac{2}{A}\left\{r_R\left(\frac{\phi L_{i+1,j}-\phi C}{\Delta XR_{i,j}+\Delta XL_{i+1,j}}\right) - r_L\left(\frac{\phi C-\phi R_{i-1,j}}{\Delta XR_{i-1,j}+\Delta XL_{i,j}}\right)\right\} + \frac{2}{B}\left\{r_C\left(\frac{\phi B_{i,j+1}-\phi C}{\Delta YT_{i,j}+\Delta YB_{i,j+1}}\right) - r_C\left(\frac{\phi C-\phi T_{i,j-1}}{\Delta YT_{i,j-1}+\Delta YB_{i,j}}\right)\right\} = 0 \quad (9)$$

Where:

$$A = \Delta XR_{i-1,j} + \Delta XL_{i,j} + \Delta XR_{i,j} + \Delta XL_{i+1,j}$$
$$B = \Delta YT_{i,j-1} + \Delta YB_{i,j} + \Delta YT_{i,j} + \Delta YB_{i,j+1} \quad (10)$$

And:

$$r_C = r_{i,j}$$
$$r_L = r_C - \frac{\Delta XR_{i-1,j} + \Delta XL_{i,j}}{2}$$
$$r_R = r_C + \frac{\Delta XR_{i,j} + \Delta XL_{i+1,j}}{2} \quad (11)$$

$\Delta XL_{i,j}$, $\Delta XR_{i,j}$, $\Delta YB_{i,j}$ and $\Delta YT_{i,j}$ are shown in Figure 2.

$\Delta XL_{i,j}$, $\Delta XR_{i,j}$, $\Delta YB_{i,j}$ and $\Delta YT_{i,j}$ are parameters computed for each cell near the interface depending on free surface location. As explained before, a boundary condition needs to be satisfied on free surface while solving Eqn. (5), therefore, the above parameters must be calculated in order to exactly locate

the reconstructed free surface profile with respect to the computational grid.

These parameters take different values, depending on the orientation of the interface line in a cell. Nearly ten different arrangements may occur depending on the f value and the free surface orientation. One of these arrangements in which the interface line intersects both horizontal edges of the cell is illustrated in Figure 3 ; for this case, the parameters are:

$$\begin{aligned} &\phi R_{i,j} = \phi_0 \ \ , \phi L_{i,j} = \phi_0 \\ &\phi \mathrm{T}_{\mathrm{i,j}} = \phi_{\mathrm{i,j}} \ , \phi \mathrm{B}_{\mathrm{i,j}} = \phi_{\mathrm{i,j}} \\ &\Delta XL_{i,j} = 0 \ , \Delta XR_{i,j} = R \\ &\Delta YB_{i,j} = \frac{\Delta Y_{i,j}}{2} \ , \Delta YT_{i,j} = \frac{\Delta Y_{i,j}}{2} \end{aligned} \tag{12}$$

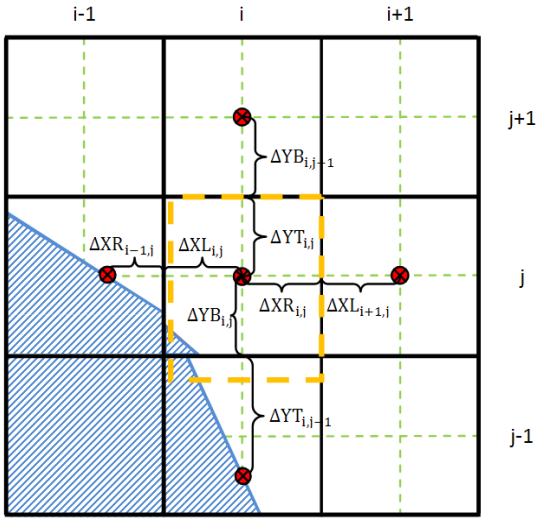

Figure 2: Nodes (red points) used to discrete the Laplace equation in a sample situation. Geometrical parameters appeared in Eqn. (9) and Eqn. (10) are also illustrated.

ϕR, ϕL, ϕT and ϕB are electric potentials used in discretization of Eqn. (5). If a node selected to discrete the equation lies on the free surface, its value is known and equal to the applied potential ϕ_0, otherwise, it must be calculated.

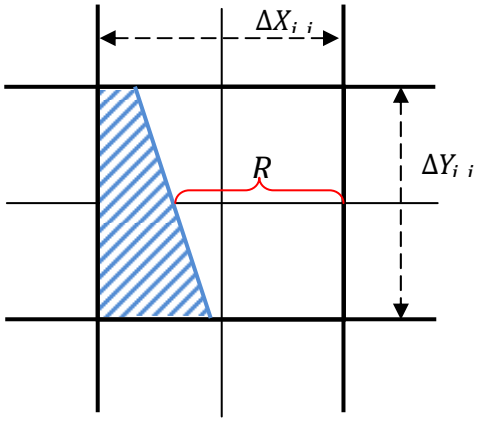

Figure 3: One orientation for the free surface where the interface line intersects both horizontal edges of the cell and one of the symmetry lines.

Electric field intensity

The electric field intensity on the free surface needs to be calculated to obtain the surface density of the electric charge and the electric force acting on the free surface. Again, an arbitrary position of the free surface on the Cartesian mesh is an issue here. As shown in Figure 4 first we find the midpoint of the approximated interface line in each cell. Then, three directions are considered: the first two being the x and y directions and the third is the direction of the line connecting the center point of the reconstructed interface line and the center of the (i+2,j+2) cell (pointed out by 'dia' subscript here as shown in Figure 4). Next the derivative of the electric potential is computed in these directions $\left(\frac{\partial \phi}{\partial x}, \frac{\partial \phi}{\partial y}, \frac{\partial \phi}{\partial n_{Dia}}\right)$. As the free surface is a boundary inside the computational domain we must use a directional derivative outward from the fluid interface. As shown in Figure 4 we select three nodes in each direction (nodes specified with red color in Figure 4), and compute the derivatives. These nodes, however, do not lie on the center of cells thus their values are initially unknown; they are calculated by interpolating between the three points. For example to find the electric potential at the red point in cell (i+2,j) of Figure 4, we use three green points as shown in the figure.

Having obtained the above derivatives, we need to calculate the electric field intensity vector by using two of the above derivatives depending on the values of f in adjacent cells.

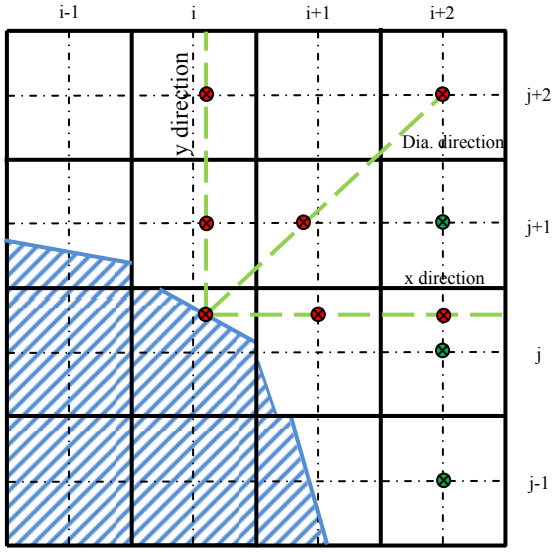

Figure 4: Nodes and directions used for the electric field intensity calculation. First, three green points are used to obtain the electric potential value at each red point (as shown symbolically for the red point within cell (i+2,j)). The red points are then used to calculate the potential derivative. (Only the three green points used to interpolate the potential value on are shown in the figure.)

RESULTS AND DISCUSSION

Although boundary condition capturing for Laplace equation on irregular domains is a conventional method [16] its integration with VOF scheme is new and presented here for the first time. So to verify the formulation and the implementation of the numerical scheme, the results are compared with the experimental solutions data.

Figure 5 shows the generic geometry of an electrowetting setup. A drop of a partially wetting conductive liquid is placed on a flat electrode, which is covered by a thin insulating layer. The liquid is typically an aqueous salt solution. Materials are chosen such that the contact angle (Young's angle) in the absence of electric field is rather large, $\theta_s > 90^{\circ}$. When a voltage is applied between the liquid and the electrode an electrostatic force acting on the free surface near the contact line makes the drop spread on the plate.

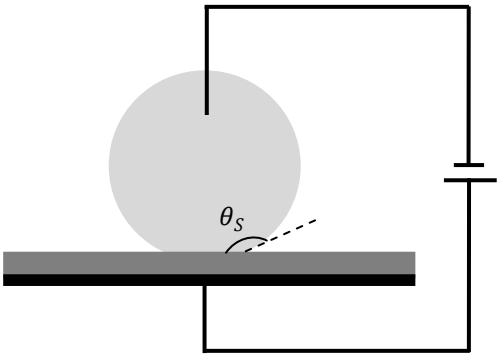

Figure 6: A conductive drop placed on an electrode covered by an insulating layer.

This phenomenon is used to pump fluid in micro scale but here we use it only to verify our models. So by assuming 150 micrometers for the insulating layer, two different voltages were applied and results were compared with experiments. In Figure 6 and Figure 7 the final drop shapes after the application of the electric field are shown, the numerical results are also indicated with solid lines in the images and a good agreement between the numerical and experimental results is obvious.

The applied potential differences are 823 volts and 1162 volts respectively. In this simulation the consequential contact angle is 170 degrees which is the same as that reported in [17]. The discrepancy on the right side of the drop in Figure 7 is due to placement of the electrode on this part instead of placing it in the middle of the drop which has spoiled the symmetry of the drop.

The reason to choose this case for verification of the numerical model is that there is no oscillating drop shape and stable state results of the drop shape are available for comparison in this experiment.

The initial shape of the drop is assumed spherical and the number of grids in the radius of the drop is 75.

Electrostatic Atomization

In the spindle mode of the electrostatic atomization, there are three different length scales:

1. The largest length scales is related to the spacing between the capillary nozzle and the electrode facing it.
2. The next length scale is that of the cone which forms at the outlet of the capillary.
3. The smallest length scale is associated with the jet departing from the vertex of the.

According to the above the largest length scale is 10^4 times greater than the smallest one and this is an issue while mesh generation for the solution domain is performed. In order to manage the problem of different length scales in the domain in this work the formation of the cone shaped part is focused on and the jet part is assumed negligible in simulation due to its negligible size in comparison with the size of the cone part.

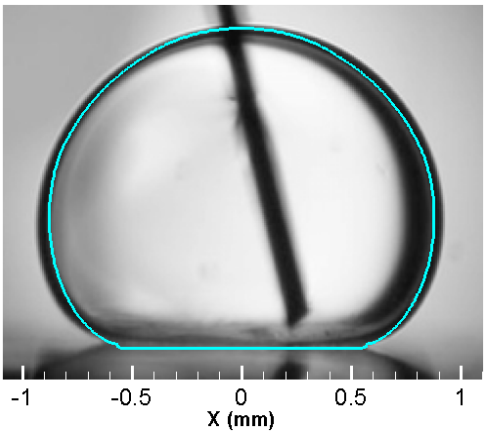

Figure 7: The final drop shape after the application of the electric field. Numerical result is indicated by the solid line. The applied voltage is 823 volts. Experimental image from [17].

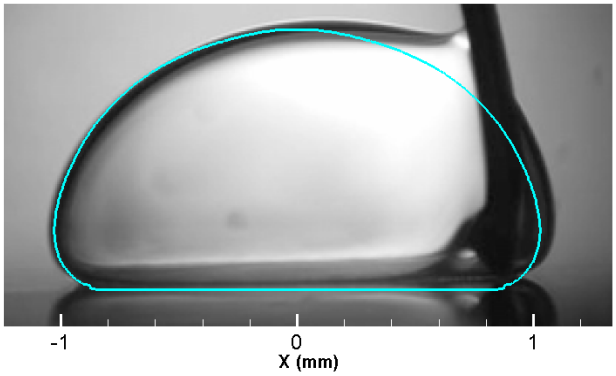

Figure 8: The final drop shape after the application of electric field. Numerical result is indicated with solid line. Applied voltage is 1162 volts. Experimental image from [17].

This assumption has no significant effect on the cone part and just decreases the accuracy of the solution at the vicinity of the

cone vertex. Then we divide the solution domain into two zones:

1. The zone in which both hydrodynamic and electrostatic equations are solved (this zone is referred to as zone 1).
2. The zone in which just electrostatic equations are solved (this zone is referred to as zone 2).

These two zones are illustrated in Figure 8. The zone defined by solid black color at the centre of the domain is the zone 1 and the rest of the domain is treated as zone 2. Uniform structured mesh is used for zone 1 and Non-uniform structured mesh is used for zone 2. The grid used for zone 2 is shown in Figure 9**Error! Reference source not found.**.

In figure 10 stages of a complete oscillation is shown. Applied voltage for this case is 3.2 KV, outside diameter of the nozzle is 510 μm and flow rate is 5 μl/min. The reference zero-point for time is the moment in which the spindle shaped part is separating from the main flow. A mesh with 60 cells lying in the outside radius of the capillary nozzle is used for this simulation.

After the separation of the spindle part at zero time the meniscus moves upward so the curvature of the free surface and consequently the surface tension force at the middle part decreases (t=0.18 ms). As a result liquid flows toward the middle point and the shape of the free surface changes to a cone again (t=0.82 ms). In this status the electrostatic forces dominate the surface tension force at the cone vertex and cause the vertex more pointed until a very narrow jet of liquid emerges from the vertex. This jet is atomized into very fine droplets at a short distance from the cone vertex. As mentioned above the jet and fine droplets leaving the cone vertex are not considered while mesh generation and assumed neglidible in simulation due to their negligible sizes in comparison with the size of the cone so they are not visible in the simulation results. Instead of this jet there are very small particles of the liquid with radiuses up to 3 cells leaving the cone vertex (t=0.98 ms). Departure of these particles stretches the vertex of the cone down and the stretched part which has a spindle-like shape separates the cone (t=1.55 ms). The length scale of this spindle-like part is greater than that of the jet and is obvious in the simulation results. There is a jet at the vertex and this jet is atomized into very fine droplets before the spindle forms.

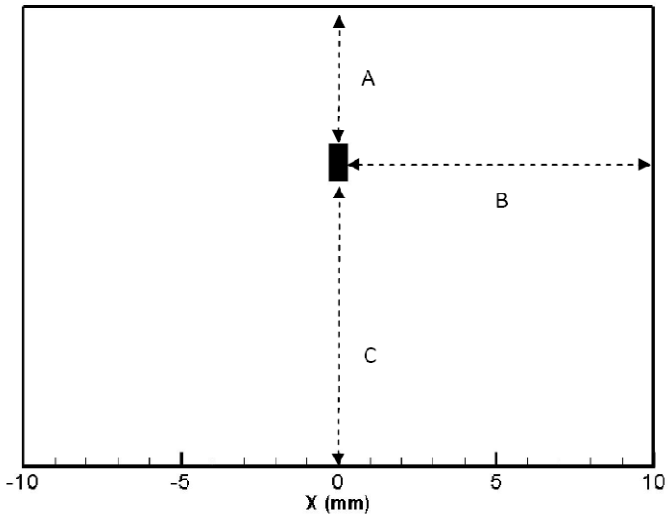

Figure 8 : The zone defined by solid black color at the centre of the domain is the zone 1 in which the hydrodynamic and electrostatic equations are solved and the rest of the domain is zone 2 in which just electrostatic equations are solved.

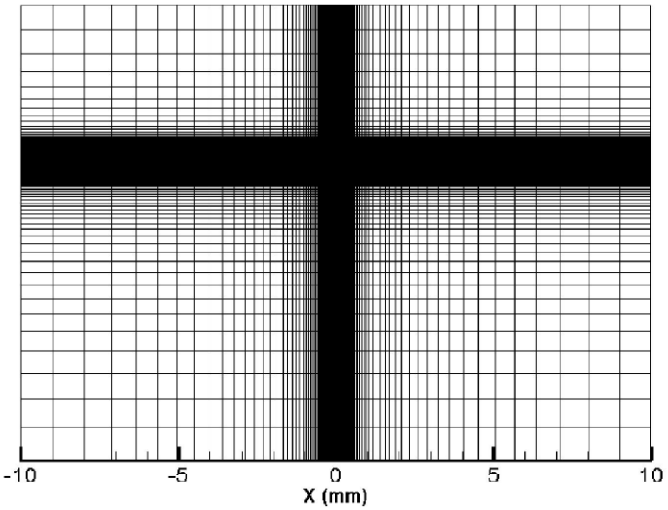

Figure 9 : The grid used for numerical calculations. Uniform structured mesh is used for the central part which is shown by a black square in figure 8 and the non-uniform structured mesh is used for the rest of the domain.

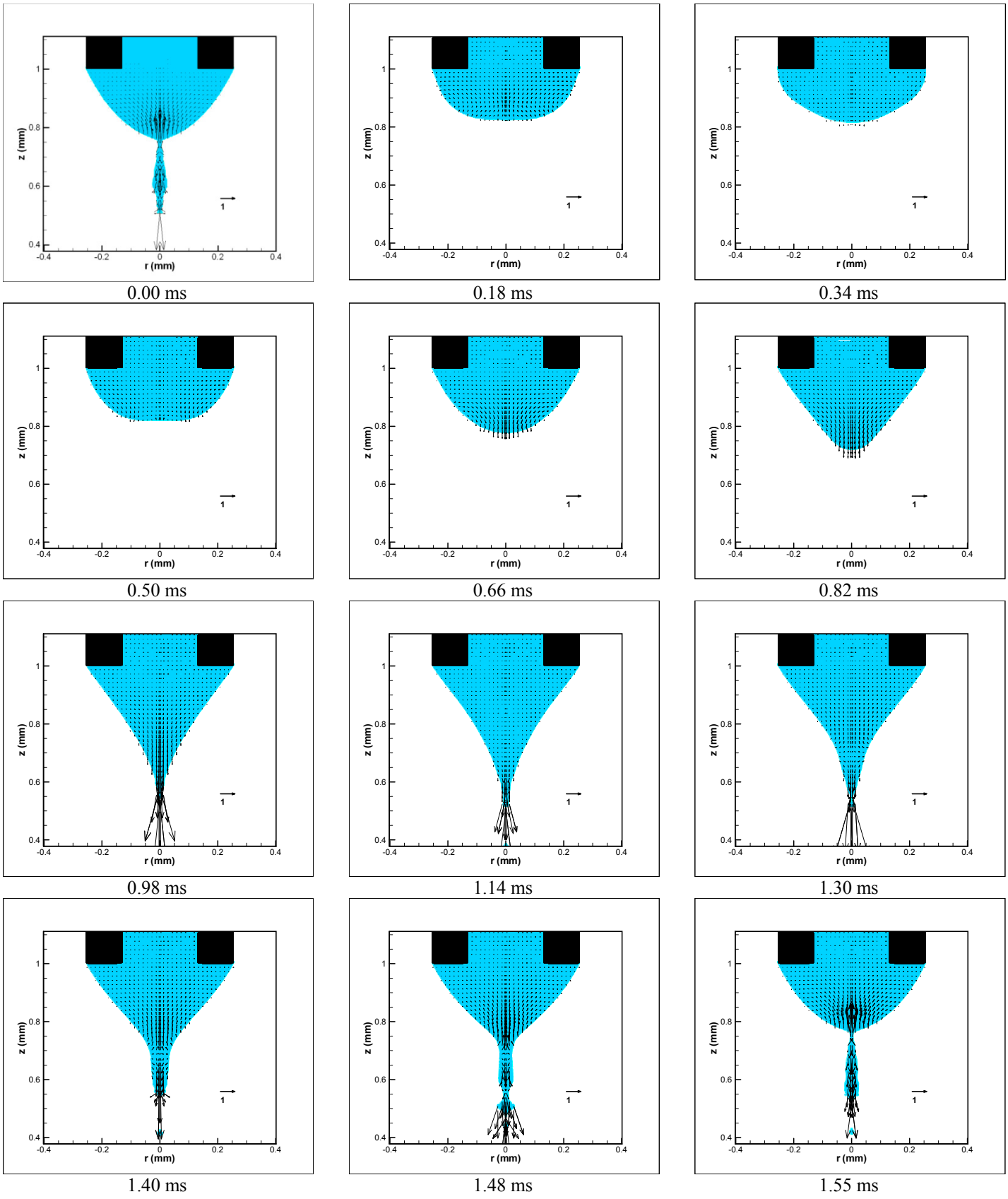

Figure 10 : The free surface shape in different stages of an oscillation in spindle mode. Applied voltage is 3.2 KV, outside diameter of the nozzle is 510 µm and flow rate is 5 µl/min.

CONCLUSIONS

In this study, the effect of the electric field on the flow of a conductive liquid with the free surface is simulated. Simulation is performed for transient state and the volume of fluid method is used to track and reconstruct the free surface. The electric field effect on the flow is due to the electrostatic forces acting on the free surface. To calculate this forces we first find the electric potential field in the solution domain and then using that calculate the electric field intensity and electric charge density and finally the electrostatic forces on the free surface. To verify the numerical results a simplified case of electrowetting phenomenon is simulated and free surface shape in stable state is compared with experimental results. The good agreement between the numerical and experimental results can demonstrate the accuracy of the model.

At last the electrostatic atomization in spindle mode is simulated using the developed code. By doing this the capability of the code to simulate the transient flows is shown. Additional results will be presented in future works.

REFERENCES

[1] Jaworek, A. and Sobczyk, A.T., 2008, "Electrospraying Route to Nanotechnology: An Overview," Journal of Electrostatics, **66**, pp.197-219.

[2] Jaworek, A. and Krupa, A., 1999, "Classification of the Modes of EHD Spraying," Journal of Aerosol Science, **30**(7), pp. 873–893.

[3] Hartman, R. P. A., Borra, J. P., Brunner, D. J., Marijnissen, J. C. M., and Scarlett, B., 1999, "The Evolution Of Electrohydrodynamic Sprays Produced In The Cone-Jet Mode, A Physical Model," Journal of Electrostatics, **47**, pp. 143–170.

[4] Hartman, R. P. A., Brunner, D. J., Camelot, D. M. A., Marijnissen, J. C. M., and Scarlett, B., 1999, "Electrohydrodynamic Atomization In The Cone-Jet Mode Physical Modeling Of The Liquid Cone And Jet," Journal of Aerosol Science, **30**, pp. 823–849.

[5] Hartman, R. P. A., Brunner, D. J., Camelot, D. M. A., Marijnissen, J. C. M., and Scarlett, B., 2000, "Jet Break-Up In Electrohydrodynamic Atomization In The Cone-Jet Mode," Journal of Aerosol Science, **31**, pp. 65–95.

[6] Alfonso, M. and Ganan-Calvo, 1998, "The Surface Charge in Electrospraying: Its Nature and Its Universal Scaling Laws," Journal of Aerosol Science, **30**, pp. 863–879.

[7] FangYan, Farouka, B. and Ko, F., 2003, "Numerical Modelingof An Electrostatically Driven Liquid Meniscus In The Cone–Jet Mode," Journal of Aerosol Science, **34**, pp. 99-116.

[8] Zeng, J., Sobek, D., and Korsmeyer, T., "Electro-Hydrodynamic Modeling Of Electrospray Ionization: CAD For A Mfluidic Device – Mass Spectrometer Interface," Flow 3D Inc.

[9] Lastowa, O., and Balachandran, W., 2006, "Numerical Simulation of Electrohydrodynamic (EHD) Atomization," Journal of electrostatics, **64**, pp. 850-859.

[10] Jackson, J. D., 1998, *Classical electrodynamics*, John Wiley and sons.

[11] Melcher, J. R., 1981, *Continuum electromechanics*, The MIT press.

[12] Berry, S., 2008, "Electrowetting Phenomenon for Microsized Fluid Devices," PhD Thesis, Tufts University.

[13] Youngs D.L., 1982, "Time Dependent Multi Material Flow with Large Fluid Distortion," Numerical Methods for Fluid Dynamics, pp. 273-285.

[14] Brackbill J.U., Kothe D.B., and Zamach C., 1992, "A continuum method for modeling surface tension," Journal of Computational Physics, **100**, pp. 335-354.

[15] Bussmann, M., 2000, "A Three-Dimensional Model of an Impacting Droplet," Ph.D thesis, University of Toronto, Toronto.

[16] Jomaa, Z., and Macaskill, C., 2005, "The Embedded Finite Difference Method for the Poisson Equation In a Domain With an Irregular Boundary and Dirichlet Boundary Conditions". Journal of Computational Physics, **202**, pp. 488-506.

[17] Mugele, F., and Buehrle, J., 2007,"Equilibrium drop surface profile in electric fields,"Journal of Physics: Condensed Mater, **19**.